Metal complexes of a novel heterocyclic benzimidazole ligand formed by rearrangement-cyclization of the corresponding Schiff Base. Electrosynthesis, Structural characterization and Antimicrobial Activity.

I. Casanova,[a] M. L. Durán,[a]* J. Viqueira,[a] A. Sousa-Pedrares,[a] F. Zani,[b] J. A. Real[c] and J. A. García-Vázquez[a]*

[a]*Departamento de Química Inorgánica, Universidad de Santiago de Compostela 15782, Santiago de Compostela Spain. E-mail: josearturo.garcia@usc.es*
[b]*Departamento di Farmacia, Parco Area delle Scienze 27/A-43124 Parma Italy.*
[c]*Institut de Ciencia Molecular Departament de Química Inorgánica, Universitat de Valencia, 46071, Valencia Spain*

Index

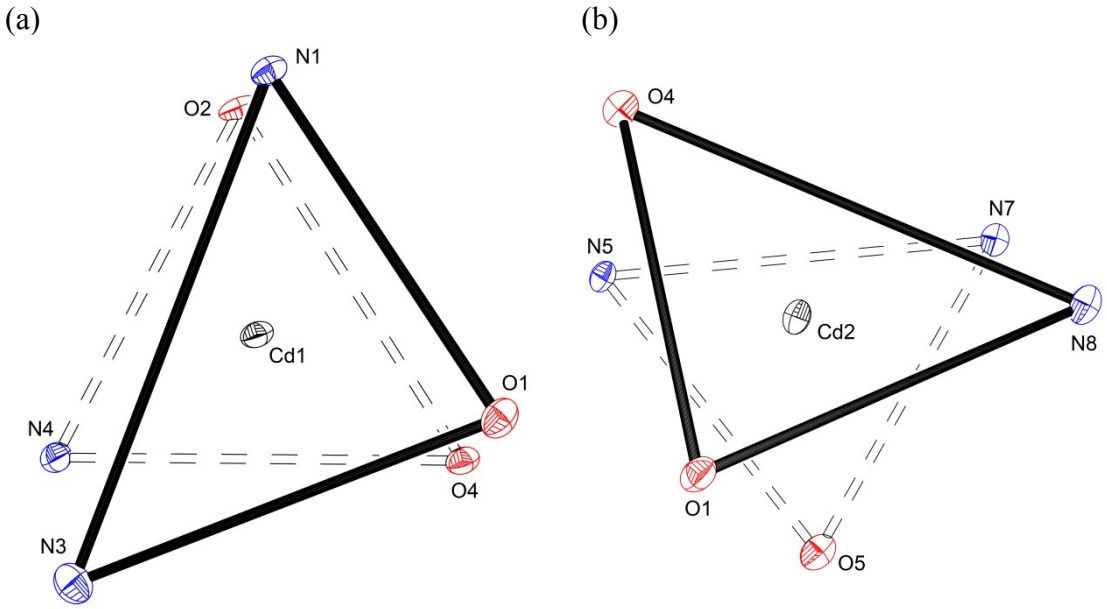

Figure S1. Scheme showing two parallel triangular faces in the six-coordinate environment of the cadmium atoms of the dimeric compound $[CdL(bpy)]_2$ **7**. The atoms are shown with 10% thermal ellipsoid probability. (a) **Cd1**. Angle between planes: 6.79(18)º.Twist angles: N1 and O1: 1.32º with O1/O4 and 7.86º with N3/N4; O1 and O4: 1.30º with N1/O2 and 22.11º with N3/N4; N3 and N4: 6.92º with N1/O2 and 21.37º with O1/O4; (b) **Cd2**. Angle between planes: 16.56(28)º.Twist angles: N5 and O4: 23.49º with O1/O5 and 28.31º with N7/N8; O1 and O5: 27.68º with N5/O4 and 39.08º with N7/N8; N7 and N8: 25.46º with N5/O4 and 30.92º with O1/O5.

Table S1 Summary of crystallographic data and refinement for compounds **1-4**[a]

Compound	**1**	**2**	**3**	**4**
Empirical formula	$C_{21}H_{12}N_2O_3$	$C_{44}H_{28}Co_2N_4O_8$	$C_{66}H_{36}Co_2N_8O_6$	$C_{255}H_{176}N_{32}Ni_8O_{33}$
Formula weight	340.33	858.56	1154.89	4685.95
Crystal size, mm	0.50x0.33x0.02	0.15x0.12x0.10	0.46x0.42x0.17	0.35x0.23x0.11
Temperature, K	293(2)	293(2)	293(2)	120(2)
Wavelength	0.71073	0.71073	0.71073	1.5418
Crystal system	Monoclinic	Monoclinic	Triclinic	Triclinic
Space group	C2/c	P2(1)/a	P-1	P-1
Unit cell dimens.				
a,Å	28.212(6)	8.0853(3)	11.7724(13)	13.0581(5)
b,Å	7.6096(17)	15.3810(4)	15.8207(18)	21.9334(9)
c,Å	14.583(3)	14.5164(4)	18.432(2)	22.0213(9)
□, °	90	90	67.749(2)	62.112(2)
□, °	106.955(4)	100.7390(10)	75.899(2)	87.140(2)
□, °	90	90	72.405(2)	73.869(2)
Volume, Å^3	2994.5(11)	1773.64(9)	2996.0(6)	5331.3(4)
Z	8	2	2	1
□, mm^{-1}	0.103	1.002	0.611	1.438
F(000)	1408	876	1180	2418
No. of reflections collected	10293	11983	27076	46717
No. of independent reflections	3061[Rint=0.0695]	4346[Rint=0.0654]	12059[Rint=0.0391]	16951 [R(int) =0.2007]
Data/restraints/parameters	3061/0/244	4346/0/267	12059/0/740	16951/2/1512
Goodness-of fit	0.846	0.969	0.893	1.049
Final R indices [I>2□(I)]	R1=0.0405	R1 = 0.0504	R1=0.0404	R1=0.0903
	wR2=0.0742	wR2 = 0.1049	wR2=0.0866	wR2=0.2434
R indices (all data)	R1=0.1488	R1 = 0.0946	R1=0.1019	R1=0.0996
	wR2=0.1015	wR2 = 0.1221	wR2=0.1052	wR2=0.2578

[a]$R1=\Sigma\{[F_o]-[F_c]/\Sigma F_o\}$. [b]$wR2=[\Sigma(F_o^2-F_c^2)/\Sigma(F_o^2)]^{1/2}$.

Table S1(cont.) Summary of crystallographic data and refinement for compounds **5-7**[a]

Compound	**5**	**6**	**7**
Empirical formula	$C_{31}H_{18}CuN_4O_3$	$C_{36}H_{24}CuN_4O_4$	$C_{66}H_{52}Cd_2N_8O_{10}$
Formula weight	558.03	640.13	1341.95
Crystal size, mm	0.45x0.37x0.07	0.40x0.20x0.10	0.48x0.17x0.12
Temperature, K	293(2)	293(2)	293(2)
Wavelength	0.71073	0.71073	0.71073
Crystal system	Monoclinic	Triclinic	Triclinic
Space group	P2(1)/c	P-1	P-1
Unit cell dimens.			
a,Å	13.703(3)	11.4821(9)	14.031(3)
b,Å	9.786(2)	12.9049(10)	14.194(3)
c,Å	20.080(4)	22.1401(17)	16.346(3)
□, °	90	92.519(2)	105.581(3)
□, °	107.637(4)	91.393(2)	100.380(3)
□, °	90	116.245(2)	110.189(3)
Volume, Å^3	2566.0(10)	2936.1(4)	2806.0(10)
Z	4	4	2
□, mm^{-1}	0.892	0.793	0.829
F(000)	1140	1316	1360
No. of reflections collected	29261	21051	15842
No. of independent reflections	5270[Rint=0.0595]	14259[Rint=0.0541]	10184[Rint=0.0451]
Data/restraints/parameters	5270/0/352	14259/0/815	10184/16/814
Goodness-of fit	0.958	0.879	0.984
Final R indices [I>2□(I)]	R1=0.0372	R1=0.0593	R1=0.0520
	wR2=0.0858	wR2=0.1184	wR2=0.1139
R indices (all data)	R1=0.0809	R1=0.1567	R1=0.0936
	wR2=0.1014	wR2=0.1486	wR2=0.1337

[a]$R1=\Sigma\{[F_o]-[F_c]/\Sigma F_o\}$. [b]$wR2=[\Sigma(F_o^2-F_c^2)/\Sigma(F_o^2)]^{1/2}$.

Table S2 Selected bond lenghts (Å) and angles (°) for **1**.

O(1)-C(1)	1.231(3)	N(1)-C(13)	1.366(3)
O(2)-C(8)	1.224(3)	N(1)-C(15)	1.370(3)
O(3)-C(17)	1.356(3)	N(2)-C(15)	1.330(3)
N(2)-C(12)	1.391(3)		
C(13)-N(1)-C(15)	107.8(2)	C(11)-C(12)-N(2)	130.4(2)

Table S3 Selected bond lenghts (Å) and angles (°) for $[CoL(MeOH)]_2$ (**2**).

Co(1)-N(1)	1.982(2)	Co(1)-Co(1)#1	3.1340(8)
Co(1)-O(4)	1.985(2)	O(1)-C(1)	1.359(3)
Co(1)-O(1)#1	2.000(2)	O(2)-C(14)	1.245(3)
Co(1)-O(1)	2.0850(19)	O(3)-C(21)	1.225(4)
Co(1)-O(2)	2.174(2)		
N(1)-Co(1)-O(4)	118.38(10)	N(1)-Co(1)-O(2)	85.29(8)
N(1)-Co(1)-O(1)#1	141.00(10)	O(4)-Co(1)-O(2)	89.66(9)
O(4)-Co(1)-O(1)#1	100.32(9)	O(1) #1-Co(1)-O(2)	100.39(8)
N(1)-Co(1)-O(1)	88.75(8)	O(1)-Co(1)-O(2)	170.63(8)
O(4)-Co(1)-O(1)	99.54(9)	O(1) #1-Co(1)-O(1)	79.80(8)

Symmetry transformations used to generate equivalent atoms: #1 -x+1,-y,-z

Table S4 Selected bond lenghts (Å) and angles (°) for **$[CoL(phen)]_2$ (3)**.

Co(1)-N(1)	2.003(2)	Co(2)-N(5)	2.138(2)
Co(1)-N(3)	2.010(2)	Co(2)-N(7)	2.141(3)
Co(1)-O(4)	2.0612(19)	Co(2)-N(8)	2.145(2)
Co(1)-O(1)	2.0831(18)	O(1)-C(1)	1.337(3)
Co(1)-O(5)	2.1723(19)	O(2)-C(14)	1.247(3)
Co(1)-O(2)	2.1817(19)	O(3)-C(21)	1.236(4)
Co(1)-Co(2)	3.1061(6)	O(4)-C(22)	1.337(3)
Co(2)-O(1)	2.0511(19)	O(5)-C(35)	1.239(3)
Co(2)-O(4)	2.0990(18)	O(6)-C(42)	1.226(3)
Co(2)-N(6)	2.134(2)		
N(1)-Co(1)-N(3)	166.17(9)	O(4)-Co(1)-O(2)	87.31(7)
N(1)-Co(1)-O(4)	102.38(8)	O(1)-Co(1)-O(2)	164.89(7)
N(3)-Co(1)-O(4)	87.04(8)	O(5)-Co(1)-O(2)	104.53(8)
N(1)-Co(1)-O(1)	86.18(8)	O(1)-Co(2)-O(4)	82.91(7)
N(3)-Co(1)-O(1)	105.19(8)	O(1)-Co(2)-N(6)	95.68(8)
O(4)-Co(1)-O(1)	83.06(7)	O(4)-Co(2)-N(6)	168.55(8)
N(1)-Co(1)-O(5)	87.76(8)	O(1)-Co(2)-N(5)	92.04(8)
N(3)-Co(1)-O(5)	85.07(8)	O(4)-Co(2)-N(5)	91.64(8)
O(4)-Co(1)-O(5)	165.22(7)	N(6)-Co(2)-N(5)	77.03(9)
O(1)-Co(1)-O(5)	86.97(7)	O(1)-Co(2)-N(7)	164.30(9)
N(1)-Co(1)-O(2)	84.55(8)	O(4)-Co(2)-N(7)	89.71(8)
N(3)-Co(1)-O(2)	85.83(8)	N(7)-Co(2)-N(8)	77.14(10)

Table S5 Selected bond lenghts (Å) and angles (◦) for [NiL(bpy)]$_2$(**4**) and [CdL(bpy)]$_2$**(7)**.

	M = Ni	**M = Cd**		**M = Ni**	**M = Cd**
M(1)-N(1)	1.963(3)	2.190(4)	M(2)-N(8)	2.082(4)	2.330(4)
M(1)-O(4)	2.094(3)	2.233(4)	M(2)-N(7)	2.075(4)	2.365(5)
M(1)-O(1)	2.055(3)	2.323(4)	M(2)-O(5)	2.113(3)	2.365(4)
M(1)-N(4)	2.060(3)	2.353(5)	O(1)-C(1)	1.350(5)	1.327(6)
M(1)-N(3)	2.117(3)	2.419(5)	O(2)-C(14)	1.249(5)	1.247(6)
M(1)-O(2)	2.137(3)	2.457(4)	O(3)-C(21)	1.239(5)	1.216(7)
M(2)-O(4)	2.040(3)	2.250(4)	O(4)-C(32)	1.332(5)	1.341(6)
M(2)-N(5)	1.967(3)	2.260(4)	O(5)-C(45)	1.256(5)	1.240(6)
M(2)-O(1)	2.109(3)	2.271(4)	O(6)-C(52)	1.232(6)	1.224(7)
N(1)-M(1)-O(1)	88.77(13)	78.95(15)	O(1)-M(2)-N(5)	95.11(12)	114.75(15)
O(4)-M(1)-O(1)	82.62(10)	75.33(13)	N(5)-M(2)-N(8)	172.83(4)	159.13(16)
N(1)-M(1)-N(4)	171.25(14)	135.24(16)	O(4)-M(2)-N(5)	87.83(12)	79.51(15)
O(4)-M(1)-N(4)	90.29(12)	87.80(15)	O(4)-M(2)-O(1)	82.62(10)	76.04(13)
O(1)-M(1)-N(4)	98.23(12)	141.61(15)	O(4)-M(2)-N(8)	97.71(12)	106.23(15)
N(1)-M(1)-N(3)	97.33(14)	110.99(16)	O(1)-M(2)-N(8)	90.13(13)	86.10(15)
O(4)-M(1)-N(3)	163.57(13)	108.24(15)	O(4)-M(2)-N(7)	89.23(13)	121.92(15)
O(1)-M(1)-N(3)	87.88(12)	83.91(15)	N(5)-M(2)-N(7)	97.15(14)	90.48(15)
N(4)-M(1)-N(3)	77.80(14)	68.79(17)	O(1)-M(2)-N(7)	165.00(13)	152.38(15)
N(1)-M(1)-O(2)	87.66(12)	76.92(14)	N(8)-M(2)-N(7)	78.47(16)	69.32(15)
O(4)-M(1)-O(2)	90.00(10)	89.47(13)	O(4)-M(2)-O(5)	173.62(11)	149.62(14)
O(1)-M(1)-O(2)	171.44(10)	132.03(13)	N(5)-M(2)-O(5)	87.88(13)	77.83(15)
N(1)-M(1)-O(4)	95.85(12)	129.80(15)	O(1)-M(2)-O(5)	93.07(11)	95.46(14)
N(4)-M(1)-O(2)	86.09(12)	80.84(15)	N(8)-M(2)-O(5)	86.95(13)	102.13(15)
N(3)-M(1)-O(2)	100.29(12)	143.63(16)	N(7)-M(2)-O(5)	95.99(13)	78.33(15)

Table S6 Selected bond lenghts (Å) and angles (°) for [CuL(bpy)](**5**) and [CuL(phen)](**6**).

	5	**6**
Cu(1)-N(1)	1.888(2)	1.889(3)
Cu(1)-O(1)	1.9164(19)	1.918(3)
Cu(1)-N(3)	2.024(2)	2.019(3)
Cu(1)-O(2)	2.0622(19)	2.101(2)
Cu(1)-N(4)	2.256(2)	2.271(3)
O(1)-C(1)	1.313(3)	1.320(4)
O(2)-C(14)	1.257(3)	1.242(4)
O(3)-C(21)	1.224(3)	1.241(4)
N(1)-Cu(1)-O(1)	91.99(9)	92.77(11)
N(1)-Cu(1)-N(3)	174.81(9)	170.69(12)
O(1)-Cu(1)-N(3)	91.02(8)	90.71(11)
N(1)-Cu(1)-O(2)	89.44(8)	88.91(11)
O(1)-Cu(1)-O(2)	169.99(9)	174.28(11)
N(3)-Cu(1)-O(2)	86.87(8)	86.83(11)
N(1)-Cu(1)-N(4)	106.98(9)	110.23(13)
O(1)-Cu(1)-N(4)	93.76(9)	102.37(12)
N(3)-Cu(1)-N(4)	77.02(9)	77.37(13)
O(2)-Cu(1)-N(4)	95.29(8)	82.14(11)

Table S7 Hydrogen bond interactions.

D-H…A	D-H (Å)	H…A (Å)	D…A (Å)	D-H…A (º)
H_2L (1)				
N(1)-H(1N)...O(1) INTRA	0.90(3)	2.31(3)	2.805(3)	114(2)
O(3)-H(2O)...N(2) INTRA	0.93(4)	1.82(4)	2.634(3)	144(3)
N(1)-H(1N)…O(1)#1	0.90(3)	2.28(3)	3.115(3)	154(2)
C(21)-H(21)…O(1)#1	0.93	2.656	3.417	139.5
$[CoL(MeOH)]_2$ (2)				
C(2)-H(2)...O(2)#1 INTRA	0.93	2.316	3.061	136.7
O(4)-H(40)…N(2)#2	0.88(4)	1.76(4)	2.641(3)	172(4)
C(17)-H(17)…O(3)#3	0.93	2.503	3.347	151.0
C(3)-H(3)…O(3)#4	0.93	2.715	3.535	147.5
$[CoL(phen)]_2$ (3)				
C(52)-H(52)...O6#1	0.93	2.347	3.130	141.7
C(47)-H(47)...N(2)#2	0.93	2.722	3.441	134.8
$[NiL(bpy)]_2$ (4)				
O(1S)-H(1S)...N(6)#1	0.84	1.92	2.734(6)	163.9
O(1SA)-H(1SA)...N(6)#1	0.84	2.01	2.725(11)	141.9
O(2S)-H(2S)...O(5S)	0.84	2.15	2.752(9)	128.7
O(3S)-H(3S)...N(102)#2	0.84	1.98	2.809(5)	171.7
O(4S)-H(4S)...N(106)#2	0.84	2.03	2.803(6)	152.2
O(5S)-H(5S1)...N(2)#1	0.82(2)	1.98(5)	2.737(6)	152(10)
C(29)-H(29)...O(3)#2	0.93	2.316	3.085	139.8
C(161)-H(161)...O(6)#1	0.93	2.345	3.226	157.8
C(128)-H(128)...O(103)#2	0.93	2.500	2.989	113.0
C(59)-H(59)...O(106)#2	0.93	2.635	3.496	154.3
C(54)-H(54)…O(1SA)#3 SOLV	0.93	2.547	3.465	169.2
C(124)-H(124)…O(3S)#4 SOLV	0.93	2.539	3.273	136.1
C(130)-H(130)…O(2S) SOLV	0.93	2.705	3.262	119.3
C(131)-H(131)…O(2S) SOLV	0.93	2.542	3.195	127.6
[CuL(bpy)] (5)				
C(22)-H(22)...O(3)#1	0.93	2.411	3.257	151.3
C(30)-H(30)...O(1)#2	0.93	2.332	3.255	171.6
[CuL(phen)] (6)				
C(22)-H(22)...N2#1	0.93	2.472	3.371	162.6
C(24)-H(24)...O(4)#2	0.93	2.655	3.454	144.6
C(31)-H(31)...O(3)#3	0.93	2.7.1	2.955	96.5
C(50)-H(50)...N(6)#4	0.93	2.536	3.449	167.3
C(55)-H(55)...O(6)#5	0.93	2.579	3.204	125.0
C(3s)-H(3s1)...O(6)#5	0.96	2.706	3.408	130.5
C(65)-H(65)...O(1)#6	0.93	2.697	3.414	134.5
$[CdL(bpy)]_2$ (7)				
O(1S)-H(1S)...N(6)	0.82	1.96	2.731(7)	155.6
O(2S)-H(2S)...O(3S)	0.82	2.08	2.825(12)	150.5
O(3S)-H(3S)...O(1S)	0.82	2.02	2.827(13)	168.0
O(3SA)-H(3SA)...O(1S)	0.82	1.81	2.582(13)	157.3
O(4S)-H(4S)...N(2)#1	0.82	2.01	2.828(9)	171.8
O(4SA)-H(4SA)...N(2)#1	0.82	2.25	2.915(17)	139.1
C(53)-H(53)...O(6)#2	0.93	2.670	3.266	122.6

C(54)-H(54)...O(6)#2	0.93	2.614	3.225	123.8
C(55)-H(55)...O(3)#3	0.93	2.522	3.208	130.8

Symmetry transformations:
(**1**) #1: -x, y, 1.5-z. (**2**) #1: 1-x, -y, -z; #2: 1.5-x, -0.5+y, -z; #3: 1.5-x, -0.5+y, 1-z; #4: -0.5+x, 0.5-y, -1+z. (**3**) #1: 1-x, 2-y, -z; #2: -x, 2-y, 1-z. (**4**) #1: x, y, z+1; #2: -1+x, y, z; #3: 1-x, 1-y, 1-z; #4: 1-x, -y, 1-z. (**5**) #1: -x, 1-y, -z; #2: 1-x, -0.5+y, 0.5-z. (**6**) #1: 1-x, -y, -z; #2: -1+x, -1+y, z; #3: 1-x, 1-y, -z; #4: 1+x, y, z; #5: 2-x, 1-y, 1-z; #6: 1+x, 1+y, z. (**7**) #1: 1+x,1+y,z; #2: 2-x, 1-y, 2-z; #3: 1+x, 1+y, 1+z.

Table S8 π-π interactions.

π-π	Cg-Cg[a] (Å)	alpha[b]	beta[c]	gamma[d]	Cg(I)_J[e]	Cg(J)_I[f]
H_2L (1)						
π[C9-C14]-π[C1,C2,C7,C8,C9,C14]#2	3.5421(18)	1.53(13)	21.1	19.7	3.3354(11)	3.3037(11)
π[C9-C14]- π[C9-C14]#2	3.6424(18)	0.02(13)	24.4	24.4	3.3185(11)	3.3184(11)
π[N1,C13,C12,N2,C15]-π[C9-C14]#3	3.6371(18)	1.47(14)	21.6	22.8	3.3538(11)	3.3812(11)
π[N1,C12,C13,N2,C15]-π[C1,C2,C7-C9,C14]#3	3.8073(18)	2.80(14)	28.1	28.5	3.3470(11)	3.3583(11)
$[CoL(MeOH)]_2$ (2)						
π[C15-C20]-π[C15,C20]#5	3.675(2)	0.02(19)	23.8	23.8	3.3638(16)	3.3634(16)
$[CoL(phen)]_2$, (3)						
π[N1,N2,C7-C9]-π[N5] INTRA	3.571(2)	10.68(19)	18.4	29.1	3.1210(13)	3.3881(15)
π[N3,N4,C28-C30]-π[N8] INTRA	3.556(2)	8.37(18)	20.6	21.9	3.2983(14)	3.3275(14)
π[N1,N2,C7-C9]-π[C8-C13]#3	3.708(2)	2.40(19)	24.1	22.5	3.464(14)	3.3852(16)
π[C46-C49,C53,C54]-π[C15-C20]#4	3.750(2)	13.05(19)	13.7	3.3	3.7434(18)	3.6433(14)
$[NiL(bpy)]_2$ (4)						
π[N4,C27-C31]-π[N8,C58-C62] INTRA	3.589(3)	13.7(2)	22.9	23.4	3.2936(18)	3.307(2)
π[N1,N1,C7-C9]-π[N5,N6,C38-C40] INTRA	3.729(3)	10.5(3)	26.3	26.6	3.333(2)	3.344(2)
π[N104,C127-C131]-π[N108,C158-C162] INTRA	3.521(3)	10.7(2)	21.4	27.2	3.1323(17)	3.278(2)
π[N101,N102,C107-C109]-π[N105,N106,C138-C140] INTRA	3.710(3)	11.6(3)	22.8	27.0	3.307(3)	3.421(2)
π[C1-C6]-π[C43-C46,C51,C52] INTRA	3.811(3)	18.7(2)	23.4	28.2	3.358(2)	3.4961(19)
π[C32-C37]-π[C12-C15,C20,C21] INTRA	3.752(3)	24.2(2)	27.5	18.3	3.5621(19)	3.3289(19)
π[C101-C106]-π[C143-C146,C151,C152] INTRA	3.751(3)	19.2(3)	20.6	26.6	3.353(2)	3.512(2)
π[C132-C137]-π[C112-C115,C120,C121] INTRA	4.029(3)	30.9(3)	29.2	16.8	3.857(2)	3.518(3)
π[N3,C22-C26]-π[N104,C127-C131]#4	3.793(3)	17.5(2)	34.7	18.6	3.5952(17)	3.119(2)
π[N4,C27-C31]-π[N103,C122-C126]#4	3.777(2)	6.0(2)	27.9	22.1	3.3380(18)	3.4989(19)
π[N7,C53-C57]-π[N7,C53-C57]#5	3.696(5)	0.0(3)	25.4	25.4	3.338(3)	3.338(3)
π[N107,C153-C157]-π[N107,C153-C157]#3	4.004(4)	0.0(3)	32.0	32.0	3.397(2)	3.397(2)
π[C8-C13]-π[C115-C120]#6	3.635(3)	3.7(3)	22.1	20.8	3.397(2)	3.369(2)
π[C12-C15,C20,C21]-π[C112-C115,C120,C121]#6	3.759(3)	2.3(2)	28.9	27.8	3.327(2)	3.2905(19)
π[C43-C46,C51,C52]-π[C139-C144]#7	3.646(3)	3.5(3)	20.9	22.1	3.378(3)	3.4052(19)
π[C39-C44]-π[C143-C146,C151,C152]#7	3.845(3)	3.3(3)	24.6	27.5	3.412(2)	3.495(2)
π[C46-C51]-π[C139-C144]#7	3.982(4)	6.0(3)	36.4	31.7	3.389(3)	3.202(3)

[CuL(bpy)] (5)						
π[C15-C20]-π[N1,N2,C7-C9]#1	3.4589(19)	3.26(15)	11.3	14.6	3.3475(12)	3.3913(12)
π[C15-C20]-π[C8-C13]#1	3.6612(19)	0.71(14)	21.8	22.2	3.3894(12)	3.3996(12)
π[C12-C15,C20,C21]-π[C12-C15,C20,C21]#1	3.6309(18)	0.00(13)	21.7	21.7	3.3744(12)	3.3745(12)
[CuL(phen)] (6)						
π[C25-C28,C32,C33]-π[C58-C61,C65,C66]#2	3.445(3)	2.5(3)	12.5	10.5	3.387(2)	3.364(2)
π[N3, C22-C26]-π[N7,C55-C59]#2	3.584(3)	1.3(2)	19.8	19.0	3.3887(19)	3.372(2)
π[C8-C13]-π[C15-C20]#3	3.931(2)	1.76(19)	27.8	29.2	3.4309(15)	3.4760(17)
π[C12-C15,C20,C21]-π[C12-C15,C20,C21]#3	3.974(2)	0.00(17)	29.1	29.1	3.4737(15)	3.4736(15)
π[C48-C53]-π[N5,N6,C40-C42]#5	3.674(2)	6.10(19)	20.7	26.5	3.2880(15)	3.4362(15)
π[C48-C53]-π[C41-C46]#5	3.662(2)	5.74(17)	20.6	24.7	3.3271(14)	3.4270(15)
π[C45-C48,C53,C54]-π[C45-C48,C53,C54]#5	3.7946(17)	0.00(12)	22.2	22.2	3.5129(12)	3.5129(12)
[CdL(bpy)]$_2$ (7)						
π[N4,C27-C31]-π[C32-C37] INTRA	3.680(4)	17.1(3)	25.0	20.5	3.448(3)	3.335(3)
π[N3,C22-C26]-π[N1,N2,C7-C9] INTRA	3.831(4)	12.5(3)	21.4	32.2	3.241(3)	3.567(3)
π[C12-C15,C20,C21]-π[C15-C20]#4	3.669(4)	2.9(3)	16.9	19.6	3.457(3)	3.510(2)
π[C8-C13]-π[C15-C20]#4	3.830(4)	7.0(3)	25.1	30.7	3.292(3)	3.470(3)
π[C12-C15,C20,C21]-π[C12-C15,C20,C21]#4	3.969(4)	0.0(3)	27.2	27.2	3.529(2)	3.529(2)
π[N7,C53-C57]-π[N7, C53-C57]#5	3.816(4)	0.0(3)	26.6	26.6	3.411(3)	3.411(3)

[a] Centroid-Centroid distance. [b] Dihedral angle between the ring planes. [c] Angle between the centroid vector Cg(I)…Cg(J) and the normal to the plane I. [d] Angle between the centroid vector Cg(I)…Cg(J) and the normal to the plane J. [e] Perpendicular distance of Cg(I) on ring plane J. [f] Perpendicular distance of Cg(J) on ring plane I.
Symmetry transformations:
(**1**) #2: -x, 1-y, 2-z; #3: -x, -y, 2-z. (**2**) #5: 2-x, -y, 1-z. (**3**) #3: 1-x, 2-y, 1-z; #4: 1+x, y, z. (**4**) #3: 1-x, 1-y, 1-z; #4: 1-x, -y, 1-z. #5: -x, 1-y, -z;; #6: 2-x, -y, 1-z; #7: 1-x, 1-y, -z. (**5**) #1: -x, 1-y, -z. (**6**) #2: -1+x, -1+y, z; #3: 1-x, 1-y, -z; #5: 2-x, 1-y, 1-z. (**7**) #4: -x, -y, 1-z; #5: 1-x, 1-y, 2-z.

Table S9 C-H...π interactions.

C-H…π	H…Cg (Å)	C…Cg (Å)	C-H-Cg (º)	D_{min} (Å)
[CoL(phen)]$_2$, (3)				
C(51)-H(51)…π[C29-C34]#4	2.917	3.768	152.8	2.955, C30
C(56)-H(56)…π[C12-C15,C20,C21]#5	2.943	3.720	142.0	3.055, C21
[CuL(bpy)], (5)				
C(25)-H(25)...π[C1-C6]#3	2.795	3.705	166.2	2.834, C2
C(23)-H(23)...π[C8-C13]#4	2.942	3.815	156.9	2.964, C9
[CdL(bpy)]$_2$ (7)				
C(22)-H(22)...π[C1-C6] INTRA	2.742	3.587	151.6	2.545, C1
C(28)-H(28)...π[N1, N2, C7-C9]#4	2.763	3.308	118.3	2.751, C9
C(56)-H(56)...π[C32-C37]#5	2.785	3.548	140.0	2.954, C32

[a] Cg: centroid; D_{min}: minimum C(H)-C(ring) distance.
Symmetry transformations: (**3**) #4: 1+x, y, z; #5: 1-x, 1-y, 1-z. (**5**) #3: -1-x, 0.5+y, -0.5-z; #4: x, -1+y, z (**7**) #4: 1-x, -y, 1-z; #5: 1-x, 1-y, 2-z.

Crystal structure of the ligand.

The structural parameters of the ligand (Table S2) are as expected. The N(2)-C(15) bond distance [1.330(3) Å] is consistent with the existence of a multiple bond character. The other N-C bond distances are in agreement with the values proposed for an N-C single bond. Similarly, the bond distances involving the ketonic oxygens atoms, O(2)-C(8) and O(1)-C(1) [1.224(3) and 1.231(3) Å] are within the accepted range for C=O double bonds, while the value of the bonding distance between carbon atom and phenolic oxygen atom C(17)-O(3) [1.356 (3) Å] is greater and consistent with the existence of a simple bond.

In the ligand (Fig. S2), the four fused rings assembly is essentially flat [r.m.s: 0.0593], as well as the phenol group [r.m.s: 0.0084]. Both planes form a dihedral angle of only 4.33 (9)° between them, so the ligand as a whole could also be considered planar [r.m.s = 0.0682].

The planar conformation of the ligand is forced by a strong intramolecular O-H…N hydrogen bond interaction established between the phenolic oxygen atom, O(3), and the imidazole nitrogen atom, N(2) (Table S7). The interaction forms a planar six-membered ring [C(15)C(16)C(17)O(3)H(20)N(2), rms: 0.087(2) Å]. The other intramolecular interaction found in the free ligand is a weaker N-H…O hydrogen bond interaction between the imidazoline nitrogen, N(1), and the quinone oxygen, O(1). This interaction is forced by the planarity of the four fused rings system (Fig. S2).

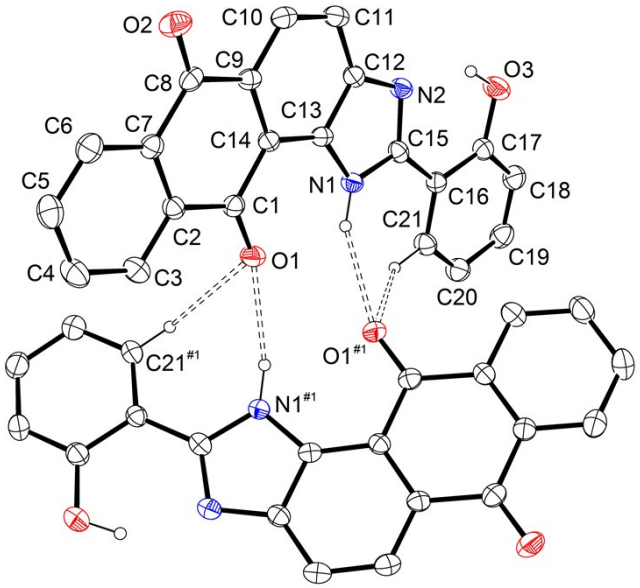

Fig. S2 Crystal packing diagram showing hydrogen bond interactions for **1**.

The crystal packing of the ligand is mainly determined by hydrogen bond interactions and by π-stacking interactions. The NH group is involved in an intermolecular N-

H…O interaction (data in Table S7) with a ketonic oxygen atom of a neighboring molecule, O(1)#1. This strong interaction gives rise to supramolecular dimers. The formation of the dimer is also reinforced by a weaker non-classical C-H…O hydrogen bond interaction, as shown in Figure S2 (data in Table S7).

Each molecule of the dimer is also involved in four π-stacking interactions with near molecules. Each face of the ligand establishes different π-π interactions. One face shows two equivalent π-π interactions between the two central rings of the four fused rings moiety. The other face shows two equivalent π-π interactions involving the imidazole ring. The data (Table S8) show that both type of interactions are strong "parallel displaced" interactions (Cg…Cg < 3.8 Å, slip angles beta, gamma < 25°).46 Taking into account that the molecules are arranged in supramolecular dimers, the π-stacking interactions connect dimers in planes parallel to the crystallographic BC plane, as shown in Figure S3. The connection between planes along the a axis is mainly achieved through non-directional van der Waals interactions between CH groups of the ligand.

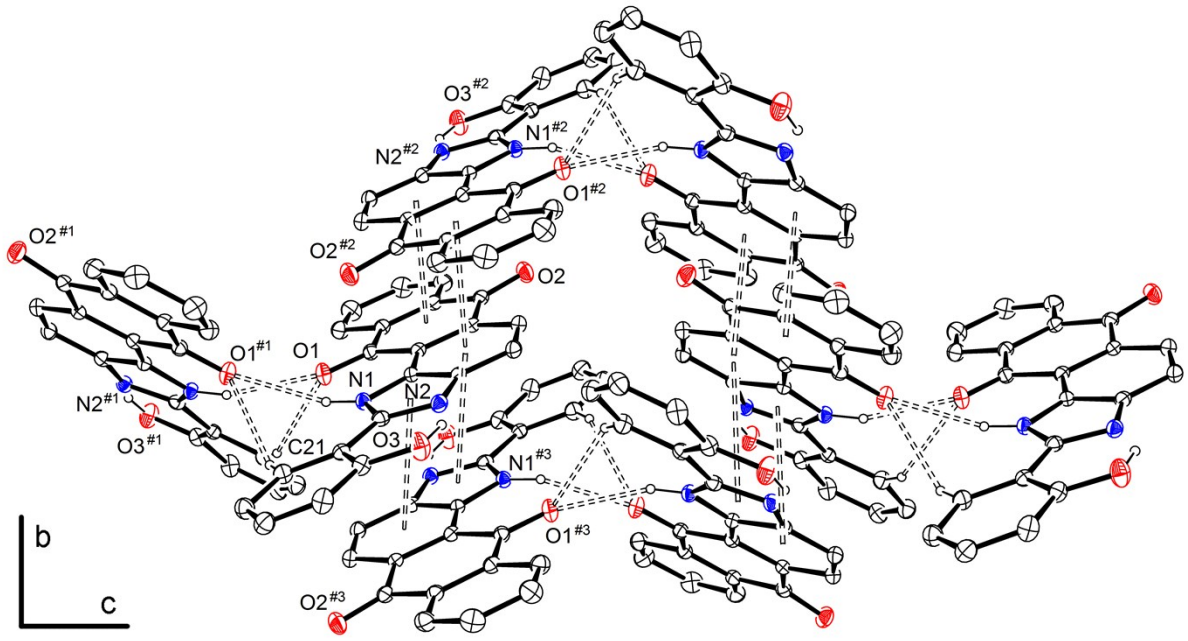

Fig. S3 Crystal packing diagram for 1 showing N-H···O intermolecular hydrogen bonds and π-stacking interactions.

Crystal packing of $[CoL(MeOH)]_2$ (2).

The asymmetrical unit of the crystal structure of $[Co_2L_2(MeOH)_2]$ contains half of the dimer (one cobalt atom, one ligand and one coordinated methanol molecule). Therefore, the intermolecular interactions for both parts of the dimer are equivalent. The strongest intermolecular interaction that determines the crystal packing of this compound is a classical

O-H…N hydrogen bond, established between the OH group of the methanol molecule, O(4), and the non-coordinated imidazole nitrogen atom, N(2), of a neighboring molecule (data in Table S7).

Each dimer is involved in four of these interactions, two as hydrogen donor and two as acceptor. Thus, these interactions connect complexes in layers parallel to the crystallographic AB plane, as shown in Figure S4.

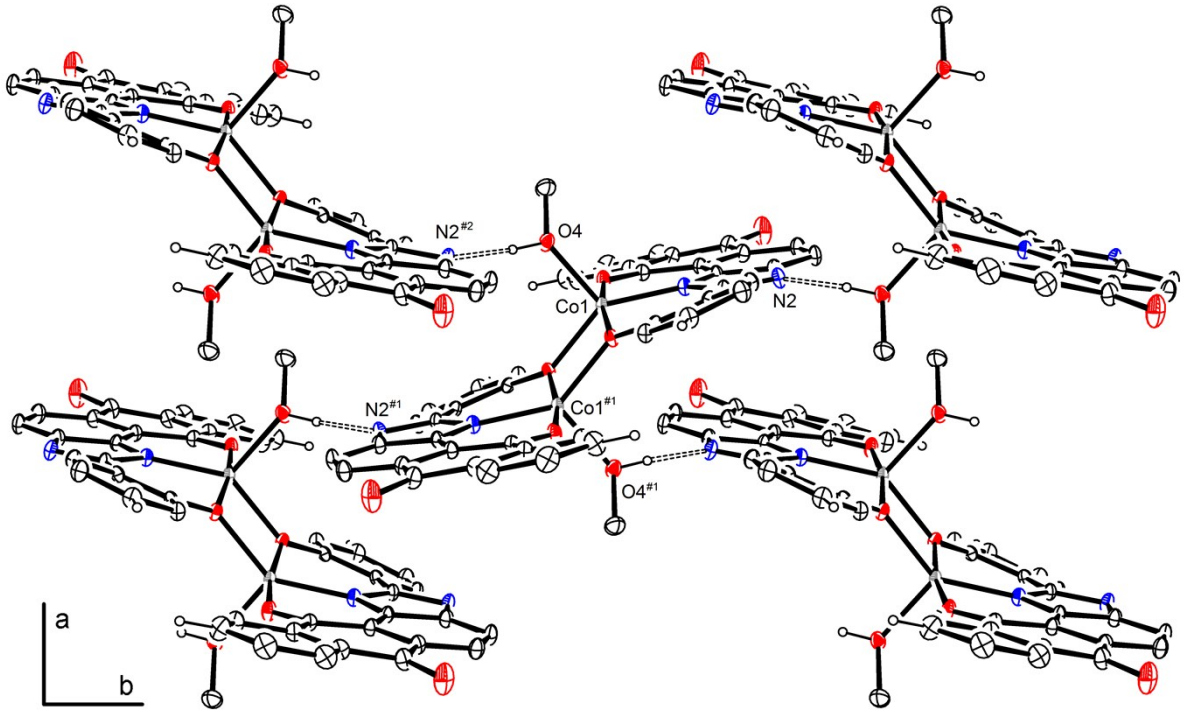

Fig. S4 Crystal packing diagram for **2** showing the intermolecular O-H···N interactions.

These layers are connected through two non-classical C-H…O hydrogen interactions and through π-stacking interactions. The C-H…O interactions connect two CH groups from the external rings of the anthraquinone ligand, C(3) and C(17), and the same oxygen atom of a non-coordinated ketone of a neighboring molecule, O(3), (data in Table S7). For symmetry reasons, these interactions occur four times per dimer (two as donor and two as acceptor). The π-stacking interactions connect the external phenyl ring of the four fused rings moiety of the ligands with its symmetry equivalent of a near molecule. These interactions occur twice per dimer. The data for these interactions (Table S8) accounts for a medium interaction. All these weaker interactions (C-H…O and π-π interactions) are located on a diagonal plane and are responsible for the cohesion of the layers parallel to the AB crystallographic plane. These interactions are shown in Figure S5.

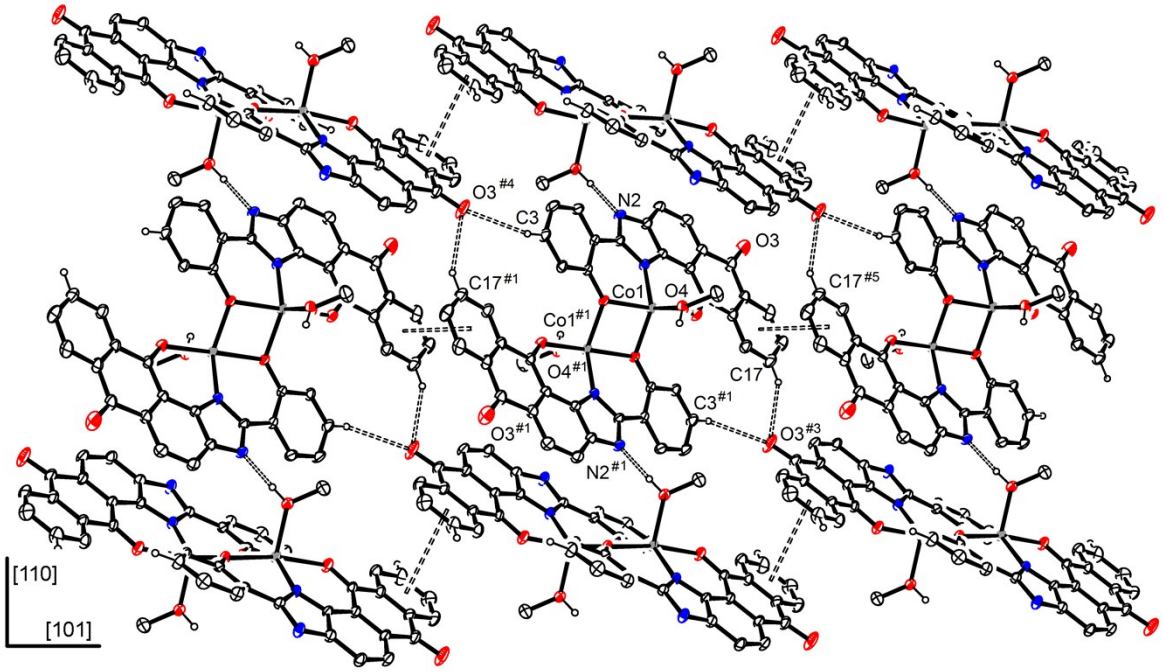

Fig. S5 Crystal packing diagram for **2** showing C-H···O intermolecular hydrogen bonds and π-stacking interactions.

Crystal packing of [CoL(phen)]$_2$ (3).

The crystal packing of this compound contains one disordered molecule of acetone per metal complex. The solvent molecules were removed using the Squeeze program (see details in the Experimental Section). However, these molecules play a role in the crystal packing, as mentioned later on.

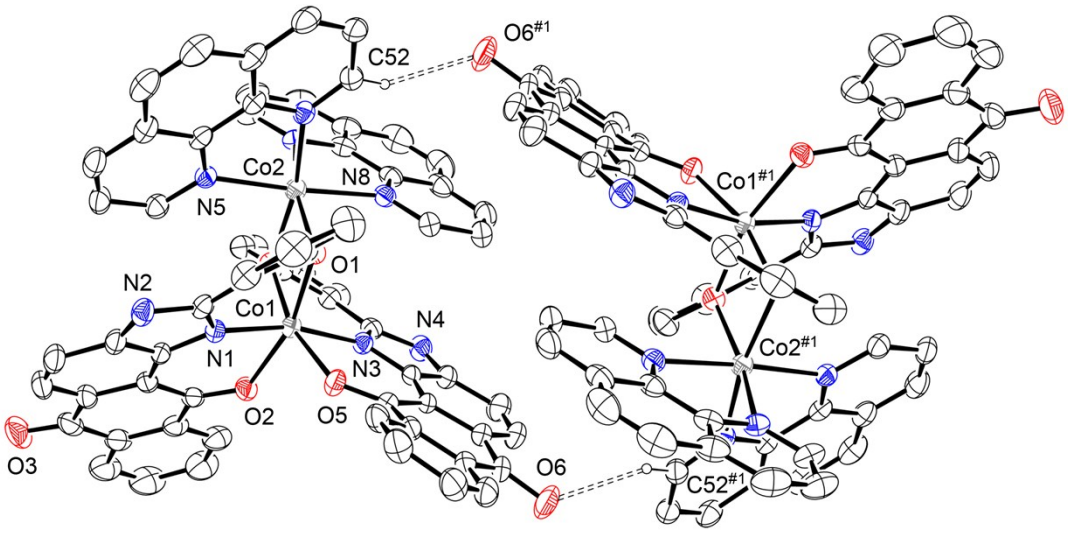

Fig. S6 Crystal packing diagram for **3** showing how C-H···O intermolecular hydrogen bonds gives rise to supramolecular dimers.

The complex presents two intramolecular π-stacking interactions between the quinone ligands and the phenanthroline coligands which influence the conformation of the molecule

(see Table S8). The complex also establishes several intermolecular interactions that are responsible for the crystal packing: two non-classical hydrogen bond interactions and two π-stacking interactions. The strongest interaction is a C-H…O hydrogen bond established between a C-H group of one of the phenanthroline coligands, C(52), and the external ketonic oxygen atom of a quinone ligand of a neighboring molecule, O(6). This interaction gives rise to supramolecular dimers, in which the complexes are related by an inversion centre (Figure S6).

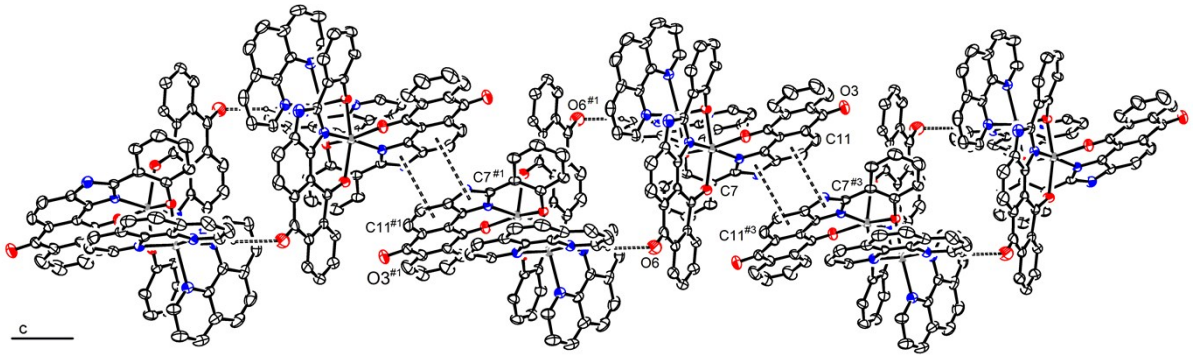

Fig. S7 Crystal packing diagram for **3** showing how C-H···O intermolecular hydrogen bonds and π-stacking interactions connecting supramolecular dimers along the crystallographic *c* axis.

The supramolecular dimers interact with neighboring dimers mainly through π-stacking interactions. The crystal packing of this compound shows two different π-stacking interactions. Each one connects dimers in one direction. One of them is a "parallel displaced" interaction between one of the imidazole rings (N1, N2) and the symmetry equivalent of its adjacent phenyl ring. This π-π interaction connects supramolecular dimers along the crystallographic c axis, as shown in Figure S7. The other stacking interaction is established between the external ring of one of the quinone ligands and the central ring of one of the phenanthroline coligads. This interaction is weaker than the previous one (see data in Table S8) and connects supramolecular dimers along the crystallographic *a* axis, as shown in Figure S8. The interaction along this direction is strengthen by a cooperative (weaker) C-H…π interaction established between a C-H group of a phenanthroline coligand, C(51), and a ring of the quinone ligand not involved in π-stacking interactions (see Fig. S8 and data in Table S9). At the crossing of both interactions (diagonal of the AC plane) another hydrogen bond is established. This is a C-H…N interaction established between a C-H group of a phenanthroline coligand, C(47), and the external imidazole nitrogen atom of a different quinone molecule of a neighboring molecule. This interaction (not shown) is much weaker than the other ones (see data in Table S9).

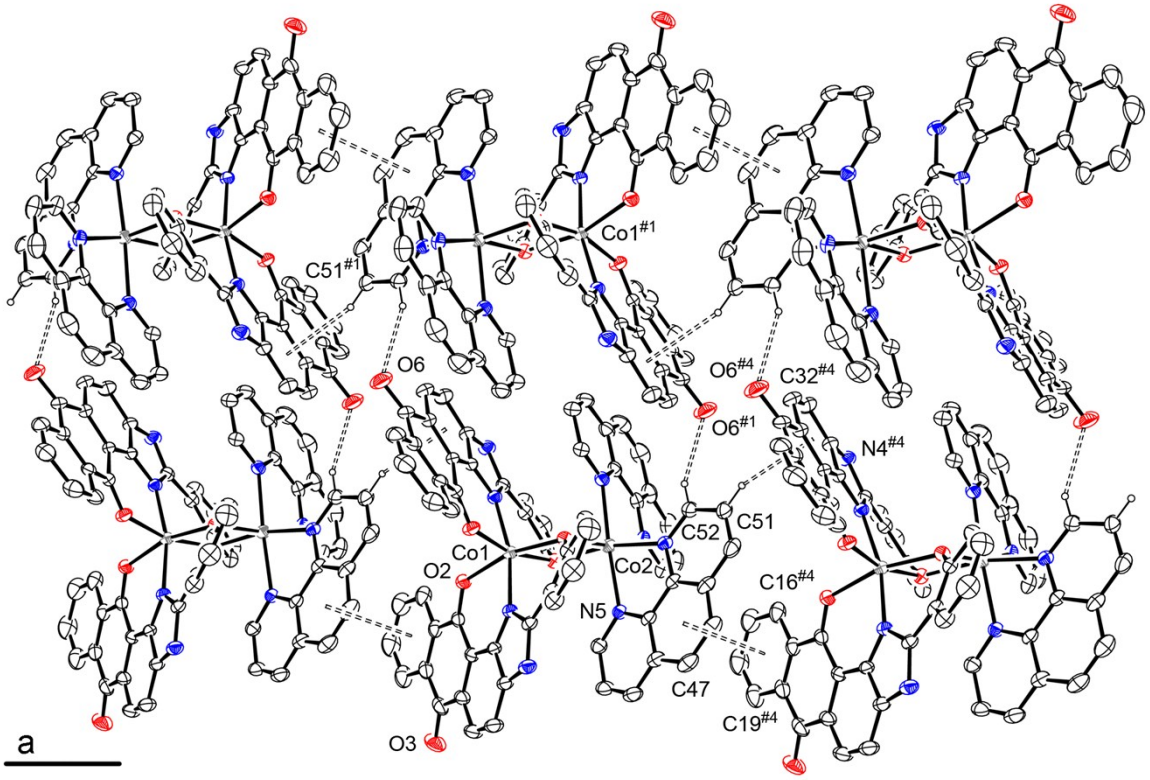

Fig. S8 Crystal packing diagram for **3** showing how C-H···π and π-stacking interactions connecting supramolecular dimers along the crystallographic *a* axis.

The strong and directional intermolecular interactions among metal complexes occur in the crystallographic AC plane. The crystal packing in the b direction involves weaker interactions, mainly non-directional. Thus, only a very weak C-H…π interaction and several non-directional van der Waals contacts can be recognized in the b direction. The C-H…π interaction is similar to the other one established in the a direction (vide supra) and connects an external C-H group of a phenanthroline coligand, C(56), and the quinone ring ligand of a near molecule. This interaction (not shown) is very weak (see data in Table S9). The acetone molecules removed from the crystal packing seem to play a role in the connection of AC layers.

Crystal packing of [NiL(bpy)]$_2$ (4).

The asymmetrical unit of **4** contains two nickel dimers, four and a half methanol molecules and one water molecule. One of the methanol molecules was severely disordered and was removed using the Squeeze program (see details in the Experimental Section). Both nickel dimers establish similar intermolecular interactions. All solvent molecules are involved in classical hydrogen bond interactions with nickel dimers. The three complete methanol molecules and the water molecule, establish O-H…N interactions with the four external

imidazole nitrogen atoms of the two dimers of the asymmetrical unit. The half methanol molecule establishes an O-H…O interaction with the water molecule. Thus, the directional intermolecular interactions involving solvent molecules do not propagate. However, the solvent molecules are involved in non-directional van der Waals contacts among molecules, influencing the crystal packing of the compound.

The structure also presents non-classical C-H…O interactions involving all the external (non-coordinated) C=O groups of the anthraquinone ligands. These interactions are established with C-H groups of bipyridine coligands of near dimers and determine the crystal packing of this compound (data in Table S7). Each dimer has two of these external C=O groups; one of them is involved in C-H…O interactions with symmetry equivalents of the same dimer and the other one is involved in C-H…O interactions with symmetry equivalents of the other dimer. The interactions involving symmetry related dimers propagate along the crystallographic *a* axis giving rise to rows of dimers. The C-H…O interactions involving non-related dimers connect these rows in the crystallographic *c* axis. Therefore, the C-H…O interactions connect molecules in layers parallel to the crystallographic AC plane. The cohesion within the layers is reinforced by weaker C-H…O interactions involving methanol molecules (O1s, O2s). These interactions are shown in Figure S9 (methanol molecules not shown).

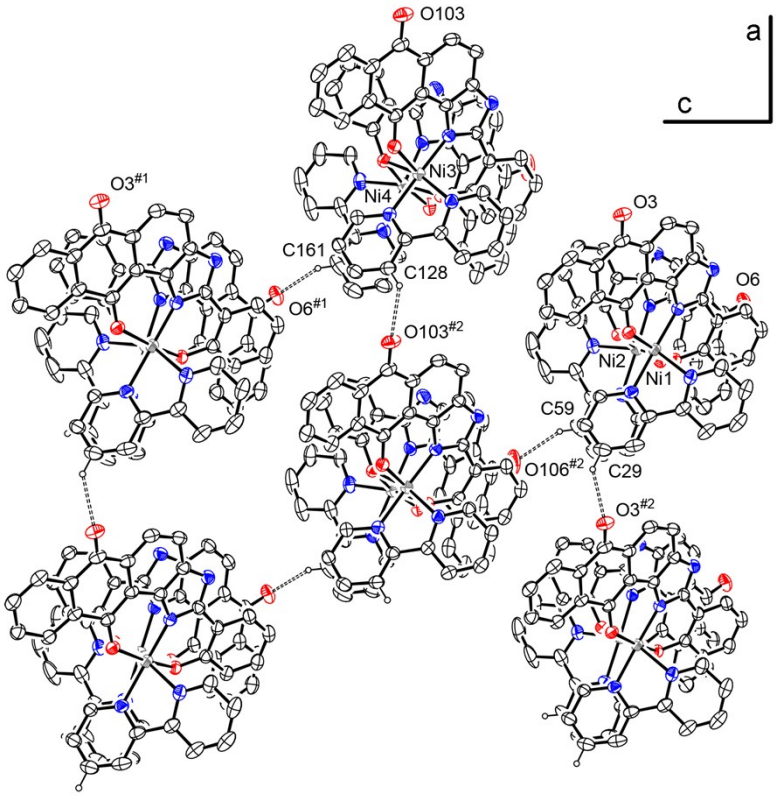

Fig. S9 Crystal packing diagram for **4** showing C-H···O intermolecular hydrogen bonds.

The connection among layers (*b* axis) is achieved by π stacking interactions. All ligands in each dimer are involved in π-π interactions. The fused rings of both anthraquinone ligands of one dimer interact with the rings of the anthraquinone ligands of the other dimer (Fig. S10). These interactions are "parallel displaced" (see data in Table S8). The bipiridine coligands are also involved in the connection among layers through π stacking interactions. Thus, one of the bipiridine ligands of each dimer establishes interactions with the symmetry equivalent of the same bipiridine ligand, while the other bipiridine ligand of each dimer establishes interactions with the other bipiridine ligand of the other dimer. These intermolecular π stacking interactions are also "parallel displaced" and of similar strength to those involving the quinone ligands (see Table S8).

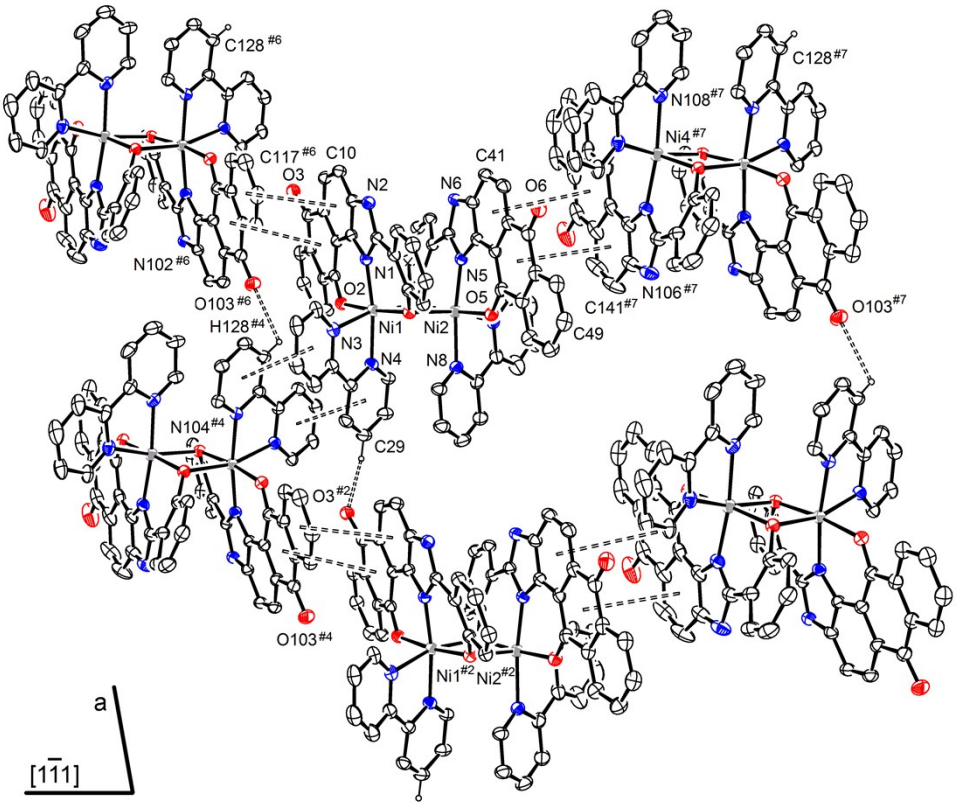

Fig. S10 Crystal packing diagram for **4** showing C-H···O intermolecular hydrogen bonds and π-stacking interactions

The ligands (anthraquinone and bipiridine) are also involved in several intramolecular π stacking interactions between them, influencing the conformation of the dimers (see Table S8).

Crystal packing of $[CdL(bpy)]_2$ (7).

The asymmetrical unit of compound **7** contains one cadmium dimer, two complete methanol molecules (O1s, O2s) and two halves of two (disordered) methanol molecules (O3s, O4s). The methanol molecules only establish strong classical hydrogen bond interactions with one

cadmium dimer or among each other. Thus, two of the methanol molecules (O1s and O4s) establish strong O-H…N hydrogen bond interactions with the external imidazole nitrogen atoms. The other two methanol molecules (O2s and O3s) establish strong O-H…O interactions with other methanol molecules (data in Table S7). Thus, the two external imidazole nitrogen atoms of the dimer are blocked with methanol molecules. This situation is similar to the one found for the nickel dimer, compound **4**, where the external imidazole nitrogen atoms were also involved in classical interactions with solvent molecules (water and methanol).

The cadmium dimers establish several directional intermolecular interactions with neighboring complexes. These interactions are C-H…O, π-π stacking and C-H…π interactions. The external non-coordinated anthraquinone oxygen atoms, O(3) and O(6), are involved in C-H…O interactions. One of them, O(6), gives rise to supramolecular dimers (Fig S11). A similar motif was previously found in the supramolecular dimers of compounds 4, 5 and 6. However, in this case the anthraquinone ligands are too far from each other to establish π stacking interactions among the anthraquinone rings (shortest centroid-centroid distance: 4.265 Å). The other C-H…O interaction, O(3), connects those supramolecular dimers along the principal diagonal of the unit cell (1 1 1), as shown in Figure 12.

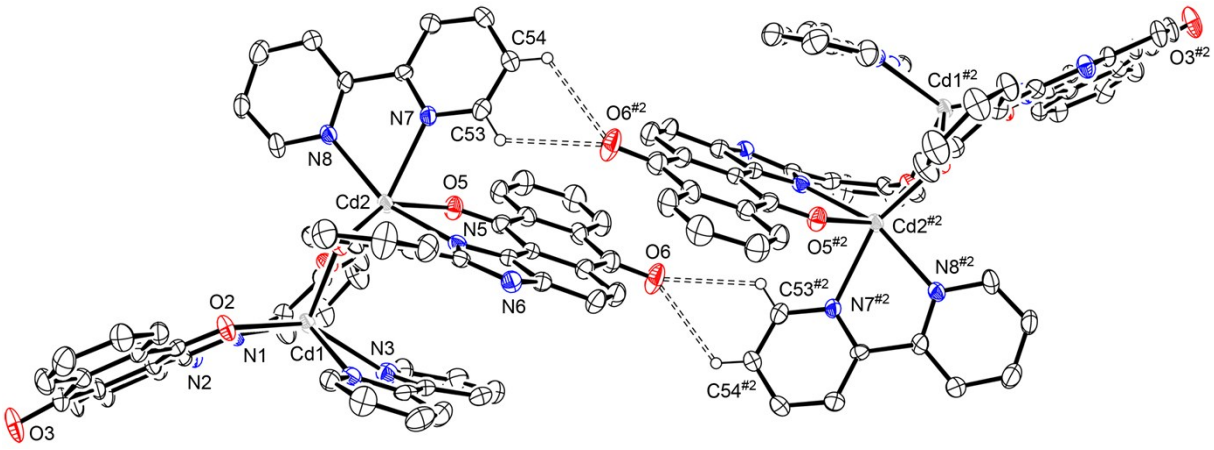

Fig. S11 Crystal packing diagram for **7** showing how C-H···O intermolecular hydrogen bonds gives rise to supramolecular dimers.

The rows of complexes along the (1 1 1) direction interact with parallel rows in the *a* direction through π stacking interactions. There are two types of π interactions in the connection between rows: strong interactions between two anthraquinone ligands and weak interactions between two bipyridine ligands, N(7) (Figure S12, data in Table S8). The propagation of these interactions forms layers of cadmium dimers in a diagonal plane. The cohesion within the layers is also reinforced by two C-H…π interactions involving CH

groups of the bipyridine coligands, C (28) and C(56), and the rings of the anthraquinone ligands (data in Table S3).

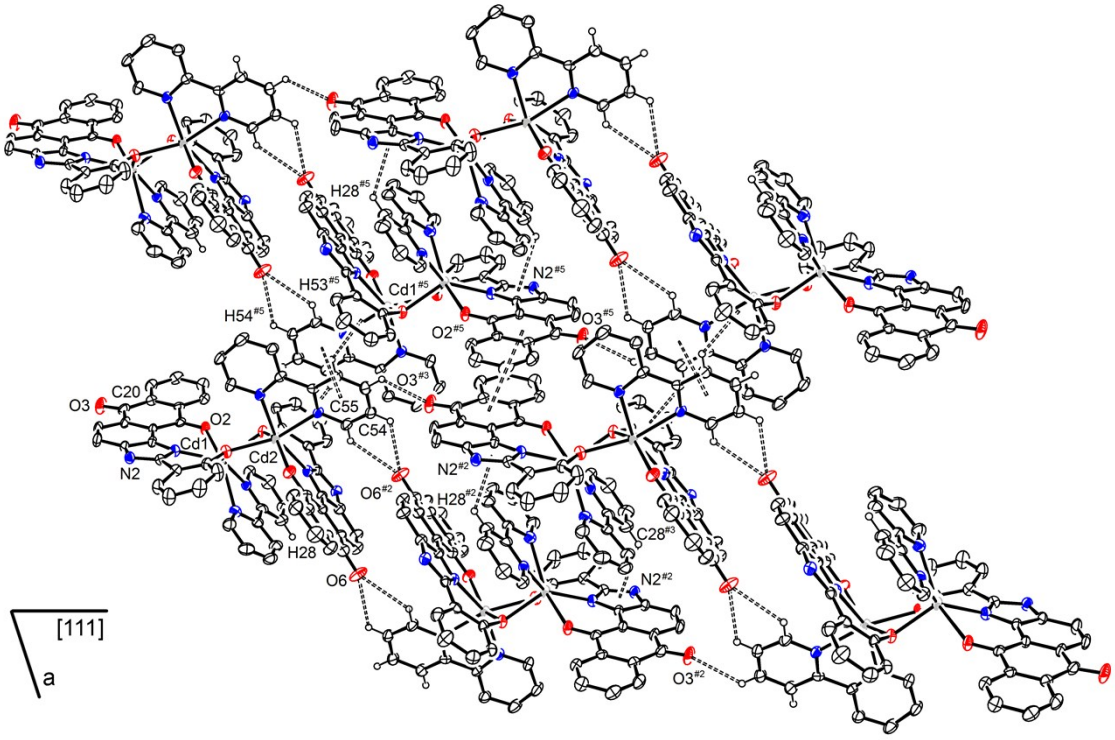

Fig. S12 Crystal packing diagram for **7** showing C-H···O intermolecular hydrogen bonds and C-H··· π and π-stacking interactions.

The connection between layers is achieved by intermolecular contacts with methanol molecules. These molecules establish strong classical hydrogen bond interactions among each other, forming a layer of solvent parallel to the layers of the cadmium complexes. This layer of solvent establishes weak C-H…O and van der Waals interactions with the layers of complexes, connecting them and completing the three dimensional structure of the crystal packing.

Crystal packing of [CuL(bpy)] (5).

The crystal packing of compound **5** contains one disordered molecule of methanol per metal complex. These molecules were removed using the Squeeze program (see details in the Experimental Section), although they are involved in the crystal packing, as mentioned later on.

Compound 5 forms supramolecular dimers with a symmetry related complex (Figure S13). The molecules in the dimer are held by C-H…O interactions involving the external C=O group of the anthraquinone ligand, O(3), (data in Table S7) and by strong π-π stacking interactions involving the three rings of the anthraquinone system. The external ring of the

anthraquinone ligand is also involved in strong π stacking interactions with the symmetry equivalent of the imidazole ring (data in Table S8).

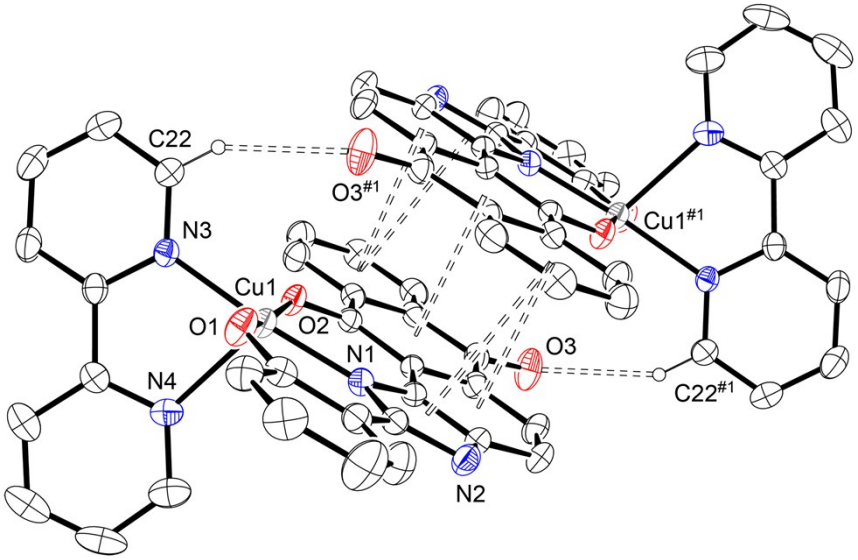

Fig. S13 Crystal packing diagram for **5** showing how C-H···O intermolecular hydrogen bonds and π-π interactions gives rise to supramolecular dimers.

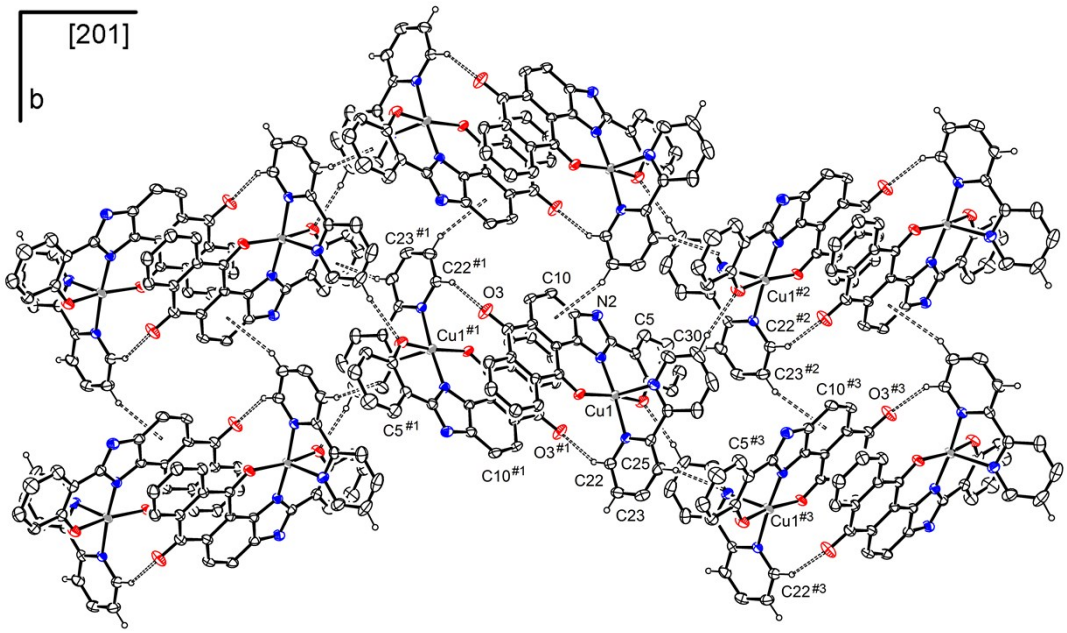

Fig. S14 Crystal packing diagram for **5** showing how C-H···O and C-H···π interactions give rise to a layer of complexes in a digonal plane.

The supramolecular dimers interact with other dimers through a strong C-H…O interaction. This interaction is established between a CH group of the bipyridine coligand, C(30), and the coordinated phenol oxygen atom, O(1). These interactions occur four times per dimer: two as (proton) donor and two as (proton) acceptor. The expansion of these interactions gives rise to a layer of complexes in a diagonal plane (see Figure S14). The

cohesion within the layers is reinforced by C-H…π interactions. These interactions connect CH groups of the bipyridine coligand, C(23) and C(25), and rings of the anthraquinone ligands of near molecules (see Figure S14 and data in Table S9).

The connection between layers is achieved by non-directional van der Waals interactions. The methanol molecules seem to be involved in the connection between those layers.

Crystal packing of [CuL(phen)] (6).

The crystal packing of compound **6** is different to the one presented by the bipyridine analog described before, compound **5**, although related.

The asymmetrical unit of **6** contains two copper complexes (Complex Cu1 and Complex Cu2) and two acetone molecules. Both compounds establish the same type of intermolecular interactions with neighboring molecules (C-H…N, C-H…O, C-H…π and π-π stacking interactions) although the crystal packing for both metal complexes is very different.

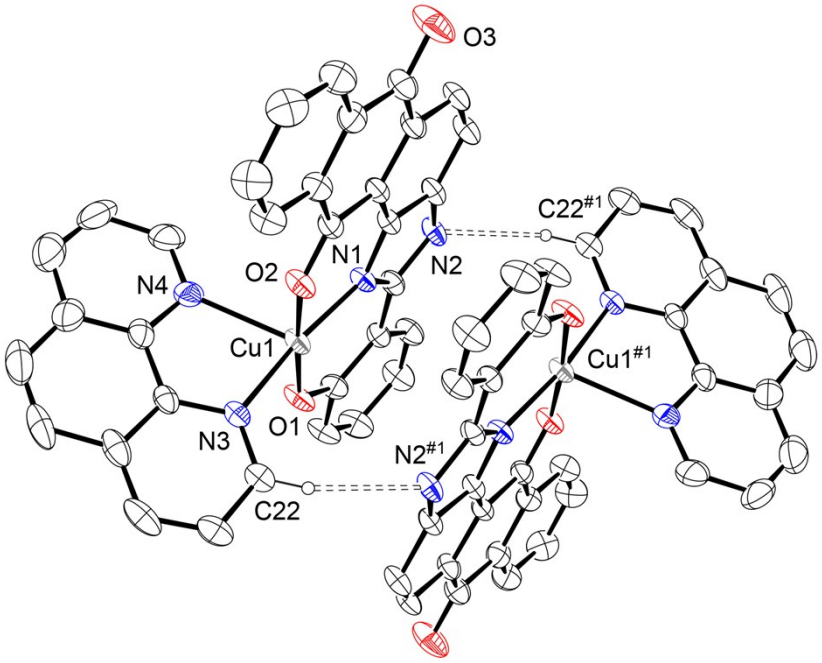

Fig. S15 Crystal packing diagram for **6** showing how C-H···N intermolecular hydrogen bonds gives rise to supramolecular dimers (Cu1...Cu1).

Each complex interacts with its symmetry equivalent forming supramolecular dimers. In the case of Complex Cu1, there are two intermolecular interactions that give rise to supramolecular dimers. (i) A strong C-H…N hydrogen bond interaction involving the external imidazole nitrogen atom, N(2), and a CH group of the phenanthroline coligand, C(22), forms supramolecular dimers in which the anthraquinone ligands are too far from each

other to establish π stacking interactions (shortest centroid-centroid distance: 4.075 Å) (Figure S15). (ii) A very weak C-H…O interaction involving the external oxygen atom, O(3), and a CH group of the phenanthroline coligand, C(31), forms supramolecular dimers that are also held together by weak π stacking interactions involving the three central rings of the anthraquinone ligand (Figure S16; data in Tables S7 and S8). The dimers described in (ii) are a recurring motif for these complexes. They are similar to the ones described before for compound 5 and to the ones formed by Complex Cu2 (see below). However, in this case the interactions that hold the dimer together are both very weak (the C-H…O is not directional and the π interactions are rather long). Thus, we will consider the dimer described in (i) as a building block for the packing, instead of (ii). This dimer will be referred to as Cu1…Cu1.

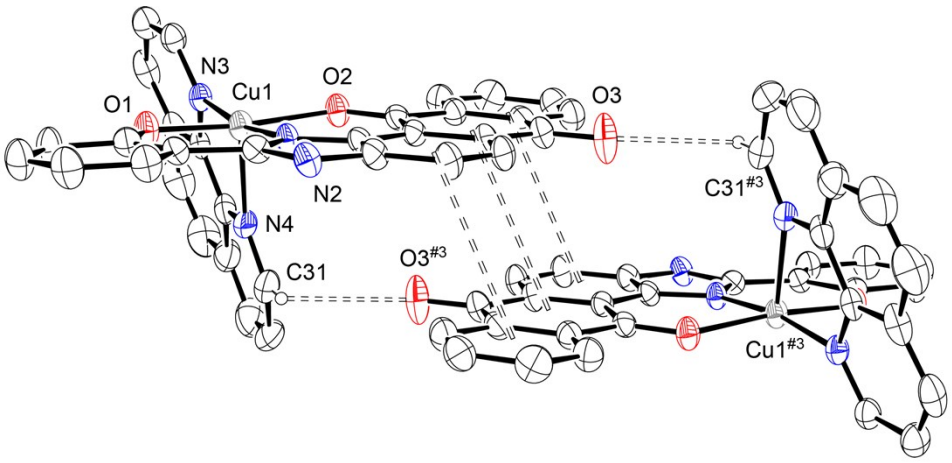

Fig. S16 Crystal packing diagram for **6** showing how C-H···O and π-π interactions gives rise to supramolecular dimers (Cu1...Cu1).

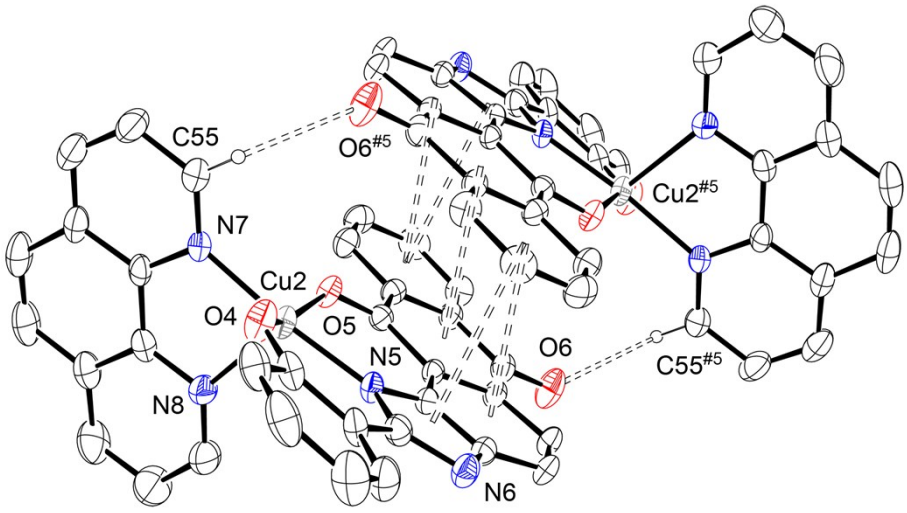

Fig. S17 Crystal packing diagram for **6** showing how C-H···O intermolecular hydrogen bonds and π-π interactions gives rise to supramolecular dimers (Cu2...Cu2).

In the case of Complex Cu2, an intermolecular C-H…O interaction gives rise to supramolecular dimers (Cu2…Cu2). The dimers are also held together by strong π stacking

interactions involving the three rings of the anthraquinone system (Figure S17; data in Tables S7 and S8). These dimers (Cu2…Cu2) are identical to the ones found in compound **5** (Figure S13).

The supramolecular dimers (Cu1…Cu1) establish intermolecular interactions with symmetry equivalent dimers along the crystallographic b axis (Figure S18). This connection is the interaction previously described for the other type of (weak) supramolecular dimers. Thus, the interactions in this direction are weak C-H…O interactions involving the external oxygen atom of the anthraquinone moiety, O(3), and weak π-π stacking interactions involving the three rings of the anthraquinone system (see data in Table S8). This row of supramolecular dimers (Cu1…Cu1) interacts with dimers (Cu2…Cu2) along the [1 1 -1] diagonal direction. The connection is achieved by weak C-H…O and strong π-π interactions. The C-H…O interactions connect C-H groups of phenanthroline coligands, C(24) (Complex Cu1) and C(65) (Complex Cu2), with coordinated phenolate oxygen atoms, O(1) (Complex Cu1) and O(4) (Complex Cu2). The strong π-π interactions occur between the same phenanthroline coligands involved in the C-H…O interactions (Figure S18), connecting copper complexes along the [1 1 -1] direction.

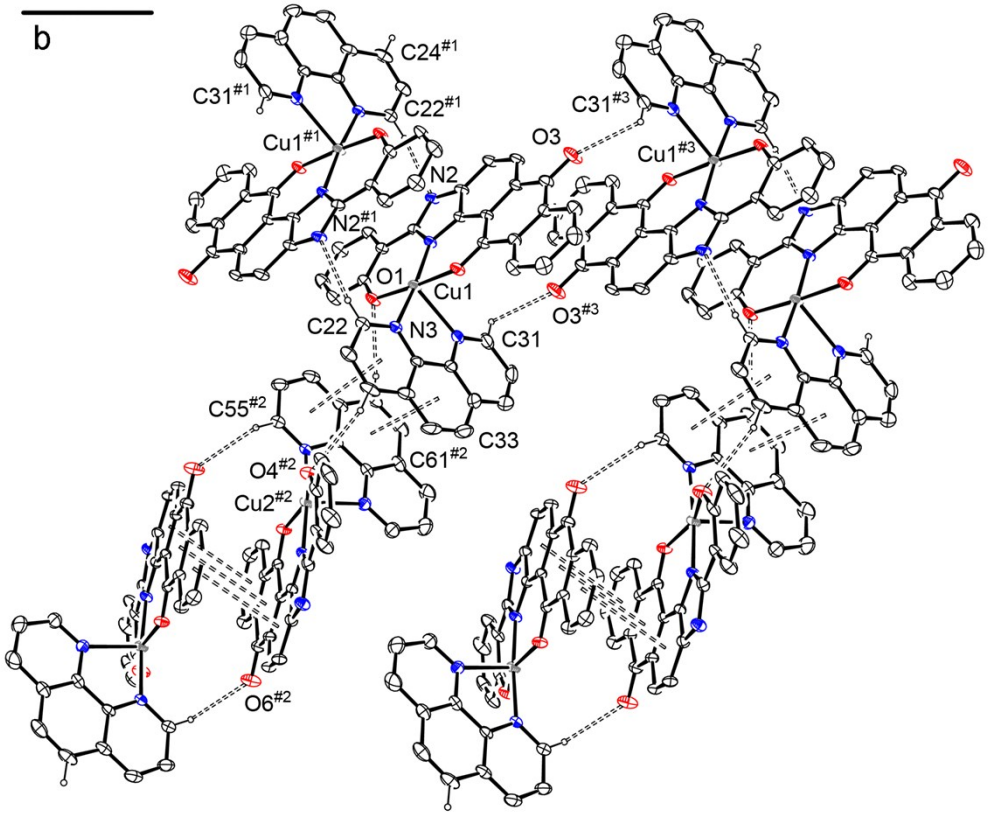

Fig S18 Crystal packing diagram for **6** showing how C-H···π and π-stacking interactions connecting supramolecular dimers along the crystallographic b axis.

The supramolecular dimers (Cu2…Cu2) establish very strong C-H…N intermolecular interactions with symmetry equivalent dimers. These interactions involve a C-H group of the anthraquinone ligand, C(50), and the non-coordinated imidazole nitrogen atom, N(6), and propagate along the crystallographic *a* axis, forming rows of supramolecular dimers (Cu2…Cu2) (Figure 16). This row of supramolecular dimers (Cu2…Cu2) establishes connections with dimers (Cu1…Cu1) as described before, i.e. by C-H…O and π-stacking interactions involving the phenanthroline coligands (Figure S19).

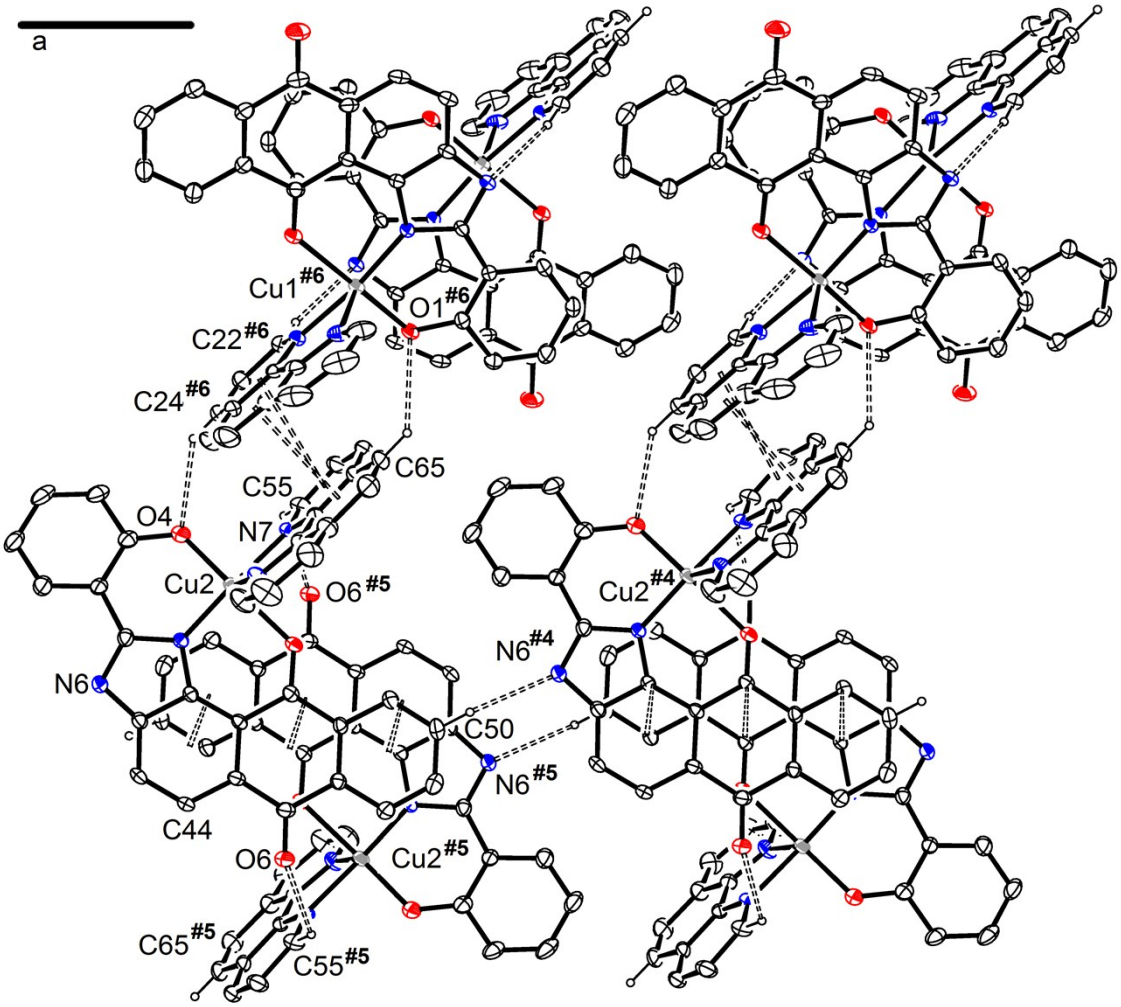

Fig S19 Crystal packing diagram for **6** showing how C-H···π and π-stacking interactions connecting supramolecnular dimers along the crystallographic a axis.

The crystal packing of this compound has voids that are occupied by the acetone molecules. These crystallization molecules interact with the complexes only by very weak C-H…O interactions (see Table S7) and by van der Waals contacts.